JCB

Article

A role for Vps1p, actin, and the Myo2p motor in peroxisome abundance and inheritance in *Saccharomyces cerevisiae*

Dominic Hoepfner,[1] Marlene van den Berg,[2] Peter Philippsen,[1] Henk F. Tabak,[2] and Ewald H. Hettema[2]

[1]Lehrstuhl für Angewandte Mikrobiologie, Biozentrum, Universität Basel, CH-4056 Basel, Switzerland
[2]Department of Biochemistry, Academic Medical Center, University of Amsterdam, 1105 AZ Amsterdam, Netherlands

In vivo time-lapse microscopy reveals that the number of peroxisomes in *Saccharomyces cerevisiae* cells is fairly constant and that a subset of the organelles are targeted and segregated to the bud in a highly ordered, vectorial process. The dynamin-like protein Vps1p controls the number of peroxisomes, since in a *vps1Δ* mutant only one or two giant peroxisomes remain. Analogous to the function of other dynamin-related proteins, Vps1p may be involved in a membrane fission event that is required for the regulation of peroxisome abundance. We found that efficient segregation of peroxisomes from mother to bud is dependent on the actin cytoskeleton, and active movement of peroxisomes along actin filaments is driven by the class V myosin motor protein, Myo2p: (a) peroxisomal dynamics always paralleled the polarity of the actin cytoskeleton, (b) double labeling of peroxisomes and actin cables revealed a close association between both, (c) depolymerization of the actin cytoskeleton abolished all peroxisomal movements, and (d) in cells containing thermosensitive alleles of *MYO2*, all peroxisome movement immediately stopped at the nonpermissive temperature. In addition, time-lapse videos showing peroxisome movement in wild-type and *vps1Δ* cells suggest the existence of various levels of control involved in the partitioning of peroxisomes.

Introduction

Eukaryotic cells are compartmentalized into organelles that execute unique and essential functions. Two classes of organelles can be distinguished based on their origin. The first class comprises the autonomous organelles such as ER, mitochondria, and chloroplasts, and the second class comprises the organelles that are derived from the autonomous organelles, such as endosomes, lysosomes/vacuole, and secretory vesicles. It is of particular importance to segregate the set of autonomous organelles properly during each cell division. This is a reflection of the accepted rule that the autonomous organelles multiply by growth and division and cannot be regenerated by de novo synthesis (Nunnari and Walter, 1996; Warren and Wickner, 1996). How do peroxisomes fit into this picture?

Peroxisomes are small single-membrane-bounded organelles containing a set of enzymes allowing them to participate in cellular metabolism (van den Bosch et al., 1992). Loss of peroxisomal function is the cause of a number of diseases in man, ranging from relatively mild single enzyme deficiencies to severe syndromes in which the biogenesis of the whole organelle is compromised (Purdue and Lazarow, 1994). The severe peroxisomal biogenesis disorders (PBDs)* are caused by a loss of protein import into peroxisomes, marking most of the PBDs as "protein-trafficking" diseases. The identification of a large number of proteins required for trafficking of peroxisomal proteins now forms the basis for a detailed molecular analysis of the import process (Hettema et al., 1999; Subramani et al., 2000). In contrast, not much data are available as to how peroxisomes multiply and are inherited upon cell division. Current opinion holds that peroxisomes multiply by growth and subsequently divide by fission, and also that they constitute a branch of the autonomous organelle fam-

*Abbreviations used in this paper: CFP, cyan fluorescent protein; GFP, green fluorescent protein; Lat-A, Latrunculin A; PBD, peroxisomal biogenesis disorder; PTS1, peroxisomal targeting signal type I; SPB, spindle pole body; YFP, yellow fluorescent protein.

ily and are segregated from mother to daughter cell (Lazarow and Fujiki, 1985). More recently, however, observations suggest that a peroxisome–ER connection exists, indicating that the ER might contribute to the biogenesis of peroxisomes. It has been postulated that peroxisomes can be formed from ER membranes (Erdmann et al., 1997; Titorenko and Rachubinski, 1998; Tabak et al., 1999). Although in many cell types peroxisomes are present in appreciable numbers and a stochastic segregation principle could suffice, all the evidence obtained thus far indicates that the proper distribution of all primary organelles between mother and daughter cells depends on specialized segregation processes involving the cytoskeleton and motor proteins (Catlett and Weisman, 2000).

In fungi, two cytoskeletal systems involved in the organization, maintenance, and segregation of cellular components have been identified: microtubules and the actin cytoskeleton. Microtubules are organized by the spindle pole body (SPB), the functional homologue of the microtubule organizing center of higher eukaryotic cells. Since *S. cerevisiae* performs a closed mitosis without breakdown of the nuclear envelope, microtubules can be classified in nuclear microtubules and cytoplasmic astral microtubules (Byers and Goetsch, 1975; Byers, 1981). Nuclear microtubules are involved in assembly of a bipolar spindle and segregation of the chromosomes (Jacobs et al., 1988; Straight et al., 1997), astral microtubules function to position, move, orient, and finally segregate the nucleus between mother and daughter cell (Palmer et al., 1992; Sullivan and Huffaker, 1992; Carminati and Stearns, 1997; Shaw et al., 1997; Tirnauer et al., 1999; Hoepfner et al., 2000). Whereas polarized vesicular movement was also shown to be dependent on astral microtubules in animal cells (Rogalski et al., 1984; Schliwa, 1984; McNiven and Porter, 1986; Vale et al., 1986; Rindler et al., 1987) and filamentous fungi (Howard and Aist, 1980; Howard, 1981; Steinberg, 1998), no such involvement could be demonstrated so far in *S. cerevisiae* (Jacobs et al., 1988; reviewed by Bretscher et al., 1994).

The actin cytoskeleton in yeast consists of two different structures, patches and cables. Patches are cortical actin–rich structures that generally cluster near regions of active secretion and therefore mark sites of growth (Adams and Pringle, 1984). Cables are long bundles of actin filaments that can span the whole cell (Adams and Pringle, 1984). Both types of actin structures behave in a cell cycle–dependent manner

Figure 1. **Peroxisome morphology as seen in GFP-PTS1–labeled cells.** In wild-type cells, up to nine individual round-shaped peroxisomes of different size and signal intensity are discernible per cellular compartment. In this static picture no localization pattern is apparent. (B) Peroxisome morphology as seen in GFP-PTS1–labeled *vps1Δ* cells. The number of individual peroxisomes is significantly reduced. Most cells only carry one peroxisome. Peroxisomes appear as large tubular structures. In budded cells, the peroxisomal tubes frequently localize near the bud neck region. Five Z-axis planes spaced by 0.8 μm have been acquired and merged into one plane. (C) Dynamics of GFP-PTS1–labeled peroxisomes in wild-type cells. Before bud emergence, peroxisomes appear randomly localized (0'). After bud emergence, two to three peroxisomes localize to the growing tip and three remain in the mother cell body (10.5'). The clustered peroxisomes in the bud remain clustered at the growing tip and the peroxisomes in the mother cell maintain a relatively fixed position (36'–90'). Before cytokinesis, the peroxisomes in the bud spread and relocalize from the bud tip to the site of cytokinesis. Similar localization to the bud neck of peroxisomes can be observed in the mother cell body (141'). After cell separation, new bud emergence of the daughter cell is observed and the peroxisomes again relocalize to the growing bud tip (159'). The described characteristics can be better observed in the Video 1 (where this sequence was extracted from) and Video 2. (D) Dynamics of GFP-PTS1–labeled peroxisomes in *vps1Δ* cells. One large, round-shaped peroxisome localizes to the site of previous cytokinesis (0'). After new bud emergence, the peroxisome glides along the cell cortex to the site of the growing tip and transforms into an elongated structure that finally reaches into the bud neck and vigorously bends out of plane in the bud (25'–103'). After fission of the peroxisomal tube, two separated, round-shaped peroxisomes appear, one located in the mother and one in the daughter cell body (110'). After cytokinesis, the peroxisomes associated with the site of previous cell separation start to elongate and reposition to the new incipient bud sites (120'). After bud emergence and bud growth, the peroxisomes repeated the characteristic movements described for the previous cell cycle. The described characteristics can be better observed in the Video 3 (where this sequence was extracted from) and Video 4. Videos are available at http://www.jcb.org/cgi/content/full/jcb.200107028/DC1. Bars, 5 μm.
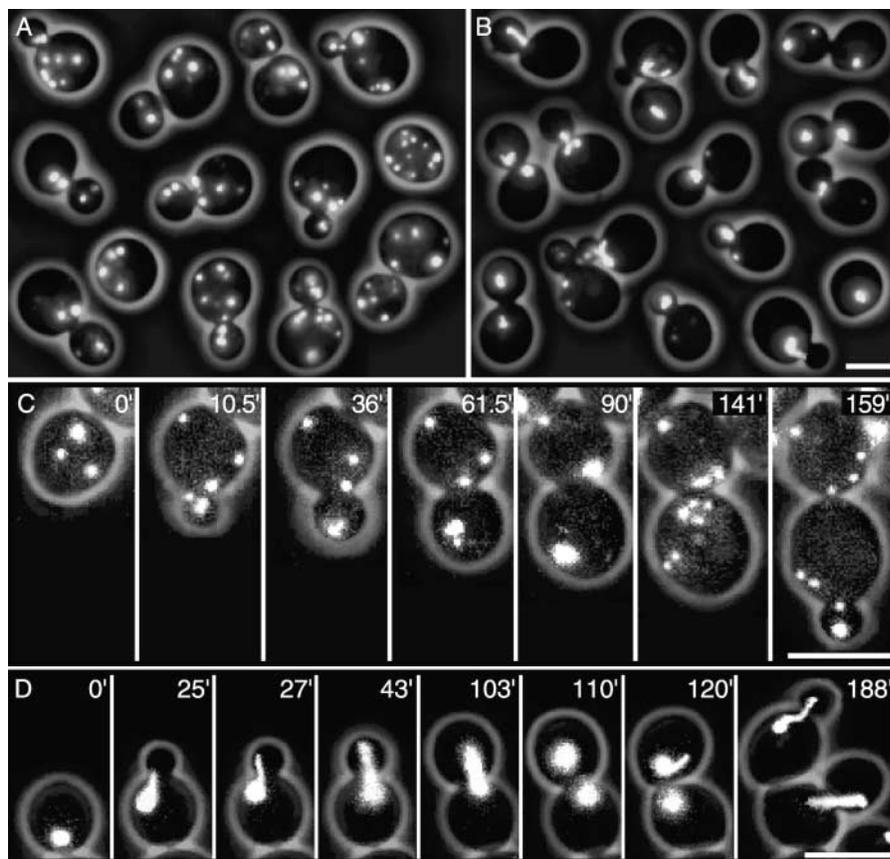
(Kilmartin and Adams, 1984; Ford and Pringle, 1991; for review see Madden and Snyder, 1998). Transport along the actin cytoskeleton of cargo such as mitochondria, vacuoles, and late Golgi compartment elements is dependent on myosin motor proteins (for review see Sellers, 2000). Myosins move in a defined directionality along the actin cytoskeleton, the polarity of which is apparent by the localization of the patches. So far, only plus end–directed myosins toward the patches have been described in *S. cerevisiae.*

In this study, we investigated the mechanisms supporting faithful inheritance of peroxisomes using in vivo time-lapse microscopy in *S. cerevisiae.* It represents a highly polarized cell in which vectorial transport of organelles and vesicles is an important feature in rapidly growing cells. We observed peroxisomal fission events and identified a mutant impaired in this process. In addition, we observed specific dynamics during peroxisomal segregation which suggests that this is a well controlled process. Furthermore, we found that peroxisome segregation requires a polymerized actin cytoskeleton and depends on the actin-associated motor protein, Myo2p.

Results

Peroxisomes segregate from mother to daughter cells

To investigate the partitioning strategy followed by peroxisomes we studied their behavior in budding yeast using time-lapse microscopy. Peroxisomes were marked with a green fluorescent protein (GFP) variant containing the peroxisomal targeting signal type I (PTS1), which is specifically imported into peroxisomes (Monosov et al., 1996; Hettema et al., 1998). Under the conditions of our experimental set up, cells contained on average 9 (3–15) fluorescent spots representing peroxisomes. Peroxisomes displayed an ordered migration behavior during the cell cycle and moved along the cortex before bud emergence (Fig. 1 A; Videos 1 and 2, with representative images shown in Fig. 1 C). A subset of peroxisomes then localized to the incipient bud site (Fig. 1 C, 0′–10.5′). These peroxisomes subsequently moved into the nascent bud as soon as a new bud was clearly visible (Fig. 1 C, 10.5′). During bud growth, peroxisome dynamics were different in the mother cell and the bud. Whereas most peroxisomes in the mother cell body retained their cortical position (Fig. 1 C, 10.5′–90′), peroxisomes in the bud displayed very complex movements. Early during the bud-growth phase, peroxisomes clustered at the bud tip and also during this phase we observed peroxisomes passing through the bud neck as observable in the second cell cycle of the mother cell in Video 2. Later during the bud-growth phase peroxisomes spread over the whole bud cortex (Fig. 1 C, 10.5′–90′). Prior to cytokinesis and cell separation, subsets of peroxisomes frequently localized to the bud neck region (Fig. 1 C, 141′, Videos 1 and 2). We conclude from these observations that peroxisomes segregate during cell division in a well-defined series of events and that the average number of peroxisomes per cell is carefully maintained. Videos are available at http://www.jcb.org/cgi/content/full/jcb.200107028/DC1.

Vps1Δ deletion mutants contain a few giant peroxisomes

Based on recent work with mitochondria, members of the dynamin protein family are likely candidates for presumptive involvement in a process supporting peroxisome fission

(van der Bliek, 1999, 2000; McNiven et al., 2000). The yeast genome contains three genes coding for dynamin-related proteins: Vps1p, Dnm1p, and Mgm1p. The deletion strains *vps1Δ*, *dnm1Δ*, and *mgm1Δ* expressing GFP-PTS1 were inspected for alterations in peroxisome morphology. Morphology and number was unaffected in *dnm1Δ* and *mgm1Δ* cells (unpublished data), however, *vps1Δ* cells showed only 1–3 peroxisomes per cell (Fig. 1 B). Moreover, the size of these peroxisomes was increased compared with those in wild-type cells (see below). To further analyze the larger GFP-PTS1–labeled structures, *vps1Δ* cells were subjected to immunogold electron microscopy using anti-GFP coupled to gold particles. Peroxisomal structures varied in morphology ranging from single enlarged organelles (un-
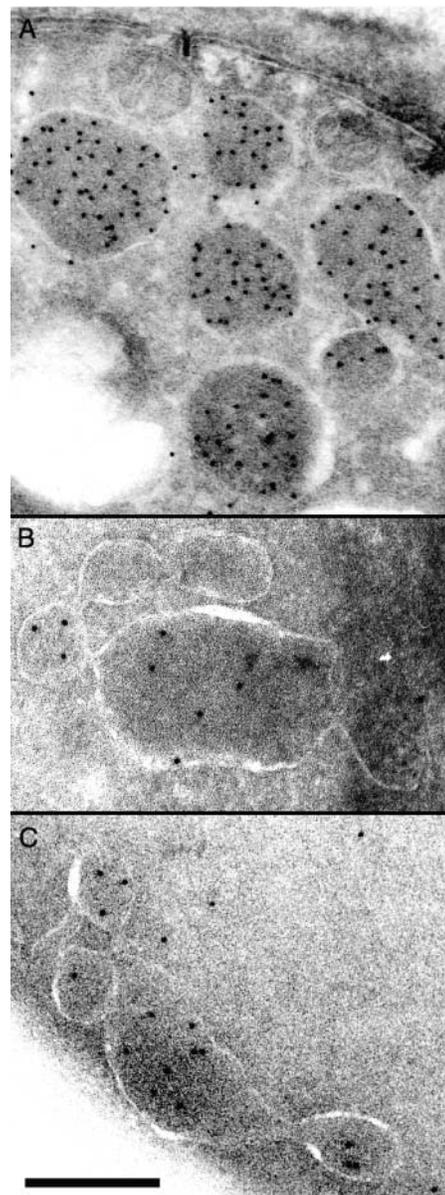

Figure 2.   **Morphology of peroxisomes in wild-type (A) and *vps1Δ* mutant cells (B and C) visualized by immunoelectronmicroscopy.** GFP-PTS1–tagged peroxisomes were identified by immunogold labeling of cryocoupes with an antibody directed against GFP. Bar, 0.5 μm.

Figure 3. **Peroxisomes and Vps1 colocalization study.** The figure shows still pictures of asynchronous cultures of CFP-PTS1–labeled peroxisomes depicted in red (A), YFP-labeled Vps1p depicted in green (B), and the overlay of the two signals (C). The phase-contrast depicting the shape of the cells is represented in blue. Five Z-axis planes spaced by 0.8 μm have been acquired and merged into one plane. Occasional overlaps of the two signals are also observed in the three-dimensional data (unpublished data). A video of images displayed in this figure is available at http://www.jcb.org/cgi/content/full/jcb.200107028/DC1. Bar, 5 μm.
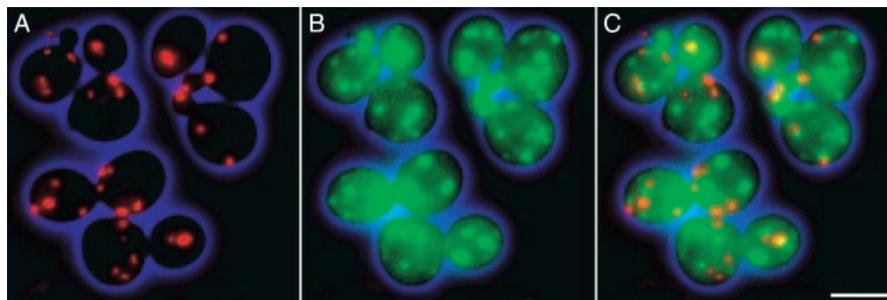
published data) to clusters and strings of small intercon-nected organelles as if they were caught in an abortive fis-sion event (Fig. 2). We propose that multiplication of peroxisomes is dependent upon Vps1p in a manner analo-gous to the function of the other dynamins involved in mi-tochondrial fission and fusion. Attempts to locate Vps1p to peroxisomes gave suggestive results, but, due to the cy-toplasmic abundance of the Vps1 protein, they remained inconclusive. For instance, association was observed in vid-eos showing coordinated movement over several minutes of patches of the yellow fluorescent protein (YFP) signal of Vps1p-YFP with the cyan fluorescent protein (CFP) signal of CFP-PTS1–labeled peroxisomes (Fig. 3 and Video 5, available at http://www.jcb.org/cgi/content/full/jcb.200107028/DC1).

Segregation of peroxisomes is accurately controlled

We were surprised that in 500 observed *vps1Δ* cells at least one peroxisome was present, although *S. cerevisiae* cells can tolerate the loss of all peroxisomes in certain *pex* mutants (Hettema et al., 2000). In vivo time-lapse imaging of 62 *vps1Δ* cells did not show a single case where insertion of at least one peroxisome into the daughter cell had failed (Vid-eos 3 and 4, representative examples extracted from Video 3 are shown in Fig. 1 D). Frequently, we observed a tubular extension emerging from a single, large peroxisome present in the mother cell which passed through the bud neck. The extension was subsequently separated from the large peroxi-

somal structure resulting in two peroxisomal structures, one in the mother cell and one in the bud.

Together, these observations in wild-type and *vps1Δ* mu-tant cells imply that peroxisomes can divide in a Vps1p-dependent and -independent manner and that their distri-bution between mother and daughter cell is not a stochastic event, but instead depends on an as yet unidentified, highly controlled segregation machinery.

Peroxisomes move independently from microtubules

Since peroxisomes were reported to be microtubule-associ-ated organelles in mammalian cells (Rapp et al., 1996; Wiemer et al., 1997), we tested whether peroxisomal move-ment depends on microtubules.

We first analyzed if peroxisomes colocalized in vivo with astral microtubules. Therefore, we used a GFP-Tub1 construct to label all microtubules (Straight et al., 1997) and YFP-PTS1 to highlight the peroxisomes (Monosov et al., 1996; Brocard et al., 1997). Although GFP and YFP could not strictly be separated by fluorescent imaging techniques, the two different structures were easily identi-fied by their typical morphology. The GFP signal of astral microtubules was very weak, preventing masking of the intensely labeled peroxisomes by the GFP signal of a mi-crotubule. We analyzed 50 cells in different cell cycle stages from log phase cultures, but no direct interactions of microtubules and peroxisomes were apparent (Fig. 4 A). To further verify that peroxisomal dynamics did not

Figure 4. **Peroxisomes and microtubules colocalization study.** Peroxisomes are labeled with YFP-PTS1 and microtubules with GFP-Tub1. The two cellular struc-tures are clearly distinguishable by their morphologies. Peroxisomes appear as dot-like structures and the spindle and astral microtubules appear as bar-like, elongated structures. (A) In wild-type cells, peroxisomes are localized in the mother cell bodies and buds and show no obvious interactions with astral microtubules. Occasional overlaps in the two-dimensional representation could not be confirmed in the three-dimensional, space-filling reconstruction (unpublished data). (B) In *spc72Δ* cells, astral microtubules that could serve as tracks to deliver peroxisomes into the bud are completely absent. Therefore, spindles appear as bar-like structures of different length, and are mislocalized and misoriented. Nevertheless, the overall localization of peroxisomes appears similar to wild-type and early bud insertion persists. Five Z-axis planes spaced by 0.8 μm were acquired and merged into one plane. Bar, 5 μm.
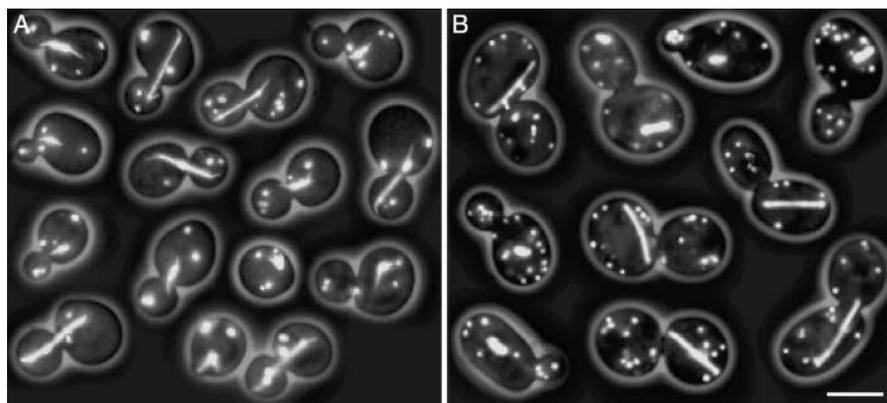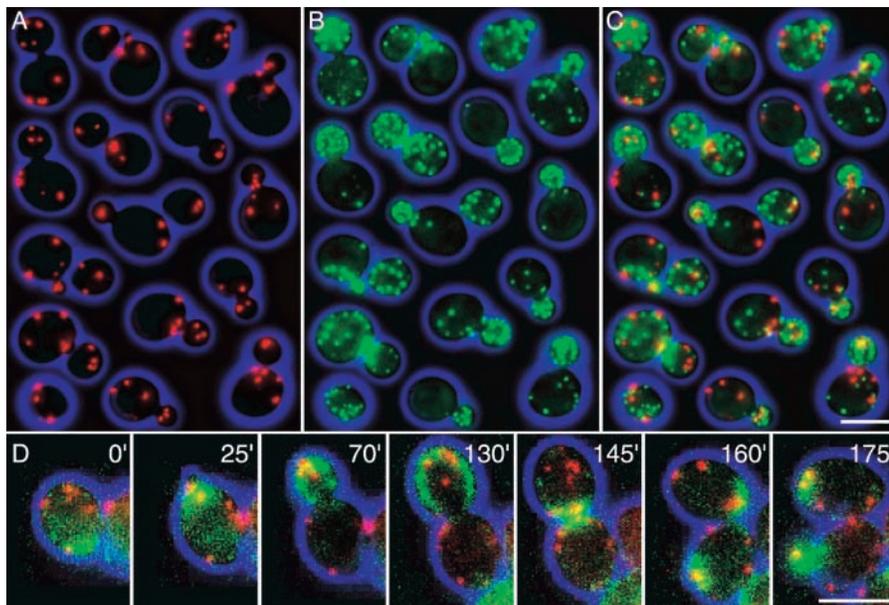
Figure 5. **Peroxisomes and actin cortical patches colocalization study.** The figure shows still pictures of asynchronous cultures with CFP-PTS1–labeled peroxisomes depicted in red (A), CAP2-YFP–labeled actin cortical patches represented in green (B), and the overlay of the two signals (C). The phase-contrast image depicting the shape of the cell is represented in blue. Five Z-axis planes spaced by 0.8 μm have been acquired and merged into one plane. Three-dimensional reconstruction (unpublished data) shows a cortical localization of peroxisomes and actin cortical patches. (D) Dynamics of peroxisomes and actin cortical patches. Actin patches start to spread from the site of the previous cytokinesis event. Peroxisomes do not show a specific cellular localization but are very dynamic at this cell cycle stage (0′). Actin patches and peroxisomes accumulate at the site of bud emergence (25′). Before the isotropic switch occurs, actin patches and peroxisomes cluster at the growing bud tip. The mother cell body is devoid of actin patches and peroxisomes in the mother cell do not exhibit significant movements (70′). After the isotropic switch occurred, actin patches start to spread all over the bud cortex. Concomitantly, the peroxisomes lose the tip localization and also start to spread along the bud cortex (130′). Actin patches accumulate at both sides of the bud neck before cytokinesis. Some peroxisomes colocalize to these actin patches (145′). After cell separation occurred, actin patches and a subset of peroxisomes relocalize to the new site of bud emergence (160′-175′). These characteristic dynamics are better observable in the Videos 6–8, available at http://www.jcb.org/cgi/content/full/jcb.200107028/DC1, where this image series was extracted from. Bars, 5 μm.

depend on astral microtubules, we analyzed *spc72Δ* cells which are unable to generate long astral microtubules (Chen et al., 1998; Knop and Schiebel, 1998; Souès and Adams, 1998). In spite of the absence of long astral microtubules and completely mispositioned and misoriented spindles, the early bud localization of peroxisomes and faithful segregation into mother and daughter cells persisted (Fig. 4 B). Initial time-lapse analysis did not reveal any characteristic alterations in peroxisome dynamics in *spc72Δ* cells compared with wild-type cells (unpublished data). Also, experiments with the microtubule inhibitors nocodazole or benomyl showed no effect on peroxisome movement (unpublished data). Together our data indicate that peroxisomes are not dependent on microtubules for vectorial movements in *S. cerevisiae*.

Directional peroxisomal movements parallel actin cytoskeleton polarity

The independence of peroxisomes on microtubules suggested the second cytoskeletal system in *S. cerevisiae* to be involved in peroxisome dynamics: the actin cytoskeleton. Therefore, we tested if the cell cycle–dependent movement and localization of peroxisomes spatially and temporally paralleled the organization of the actin cytoskeleton. To label the actin cytoskeleton, we fused YFP to the actin-capping protein Cap2, which highlights actin patches but does not label actin cables (Waddle et al., 1996). Direct GFP fusion to actin (Act1) or other proteins in order to visualize actin cables has so far not been successful (Doyle and Botstein, 1996). In addition, we labeled the peroxisomes with CFP-PTS1.

We analyzed 50 Cap2-YFP, CFP-PTS1–labeled cells in different cell cycle stages. Z-axis scans performed through the cells using Cap2-YFP as a cortical reference revealed almost exclusive cortical localization of peroxisomes; however, although the general distribution of actin patches and peroxisomes was very similar, no tight colocalization of patches and peroxisomes was apparent (Fig. 5, A–C). Nevertheless, the cortical localization and relative distribution was indicative of association of peroxisomes with actin cables. To test this hypothesis we performed time-lapse analysis of cells expressing both Cap2-YFP and CFP-PTS1 in wild-type cells. Since myosin/actin cable–based cargo movements have only been reported to occur toward the patch-covered plus end (the barbed end) in *S. cerevisiae* (Brown, 1997), we hypothesized that long range peroxisome migration on actin cables would be directed toward actin patches. To test this hypothesis, we analyzed the movement of CFP-PTS1–labeled peroxisomes relative to Cap2-labeled actin patches in 38 wild-type cells. Long range movement of actin patches (translocations >1 μm) in the mother cell body strictly followed the actin polarity (Videos 6–8, available at http://www.jcb.org/cgi/content/full/jcb.200107028/DC1; representative examples extracted from Video 6 shown in Fig. 5 D). Peroxisomes exclusively moved toward the selected bud site. In small budded cells, they generally moved toward the bud tip where they formed clusters (Fig. 5 D, 0′–70′). Although we observed oscillations back and forth, long range retrograde movement only occurred after the isotropic switch and reorientation of the actin cytoskeleton toward the mother–daughter junction, before cytokinesis (Fig. 5 D, 70′-145′). When the subsequent bud site was selected at the distal pole, the observed reorientation of the actin cytoskeleton was always accompanied by a change in the direction at which at least several peroxisomes moved. (Fig. 5 D, 145′-175′).

Figure 6. **Colocalization study of peroxisomes and actin cables in wild-type cells.** GFP-PTS1–labeled (A) log phase cells were fixed and the actin cytoskeleton stained with phalloidin-rhodamine (B) and the two channels were overlaid to check for colocalization (C). Peroxisomes in the mother cell are almost exclusively localized on actin cables. Due to the relative brightness and out-of-focus light of actin cortical patches in small buds it is difficult to determine the localization of the peroxisomes. In large budded cells, however, peroxisomes again are detectable on actin cable structures. Actin cable–based peroxisomes are especially apparent in the cell indicated with an arrow and represented in larger magnification in D. Bars, 5 µm.
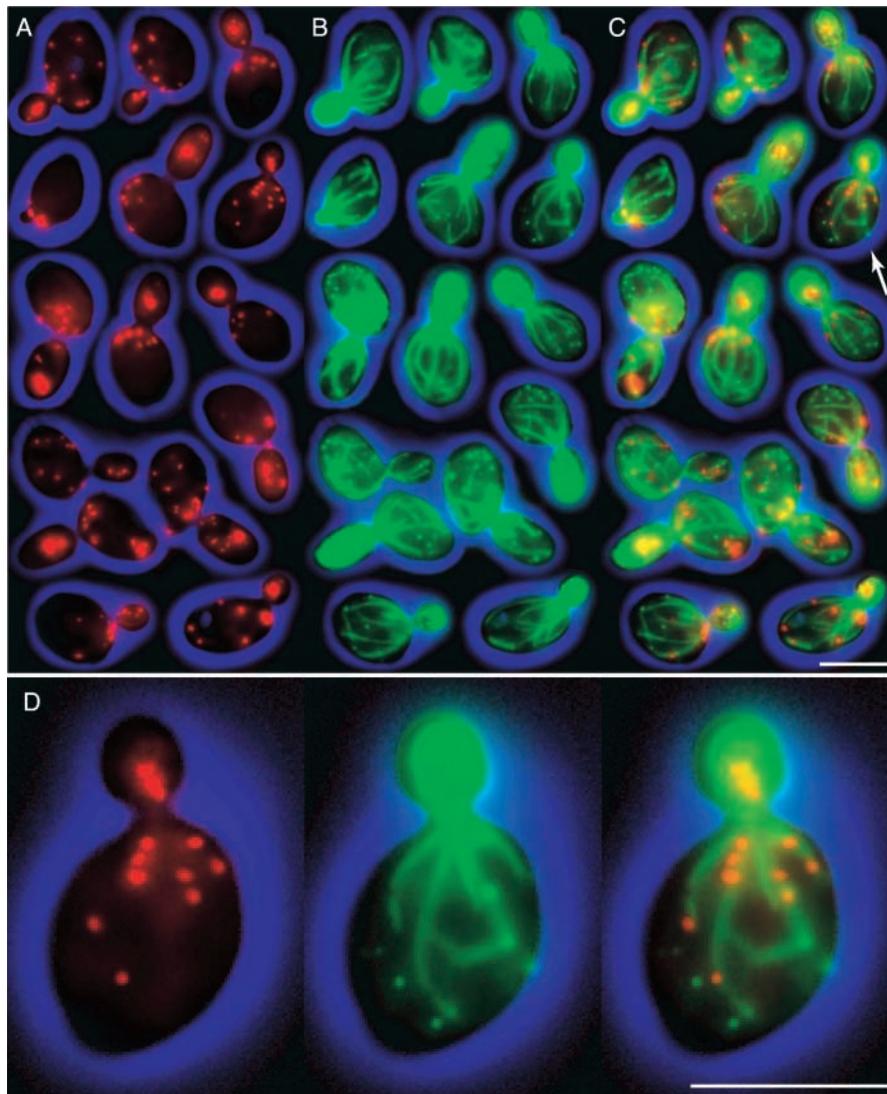
Peroxisomes colocalize with actin cables

Using a mild fixation method and staining the cells with phalloidin-rhodamine, it was possible to stain actin structures without loosing the GFP signal of stained peroxisomes (see Materials and methods and the acknowledgment). Peroxisomes in both the mother cell and in large buds before cytokinesis colocalized with actin cables (Fig. 6). In small budded cells the relatively stronger fluorescence of the actin patches in the bud unfortunately masked the lower signal of the cables and did not allow cable structures to resolve. In *vps1Δ* cells, the colocalization was even more striking as the peroxisomal tube–like extensions exactly followed one of the actin cables (Fig. 7).

Actin depolimerization abolishes peroxisomal movements

To obtain further support for actin-based peroxisomal movement we incubated GFP-PTS1-labeled cells with La-trunculin A (Lat-A). This drug sequesters actin monomers and thereby disrupts the complete actin cytoskeleton (Coue et al., 1987). As a control we used Cap2-YFP, CFP-PTS1–labeled cells. After incubation for 15 min in 200 µM Lat-A at 30°C, the Cap2 label lost its defined localization and completely dispersed throughout the cell (unpublished data). We used these conditions to study the effect of Lat-A on peroxisomal movements. We tracked movements of individual peroxisomes over 15 min in Lat-A–untreated and -treated cells (Video 9, available at http://www.jcb.org/cgi/content/full/jcb.200107028/DC1). Peroxisomal movements in Lat-A–treated cells were drastically reduced to minor oscillations in the mother cell as well as in the bud (Fig. 8).

In Lat-A–treated cells microtubule dynamics persisted whereas peroxisomal movements were completely absent (unpublished data). Together, our results demonstrate that peroxisomes colocalize with the actin cytoskeleton and that directed movement depends on a properly organized actin cytoskeleton.

Peroxisomal movement is dependent on the class V myosin Myo2

Movement along actin cables is mediated by myosin motors. In *S. cerevisiae* five myosin genes have been identified, two of class I, one of class II, and two of class V (for review see Sellers, 2000). Among these three classes, class V myosins are the
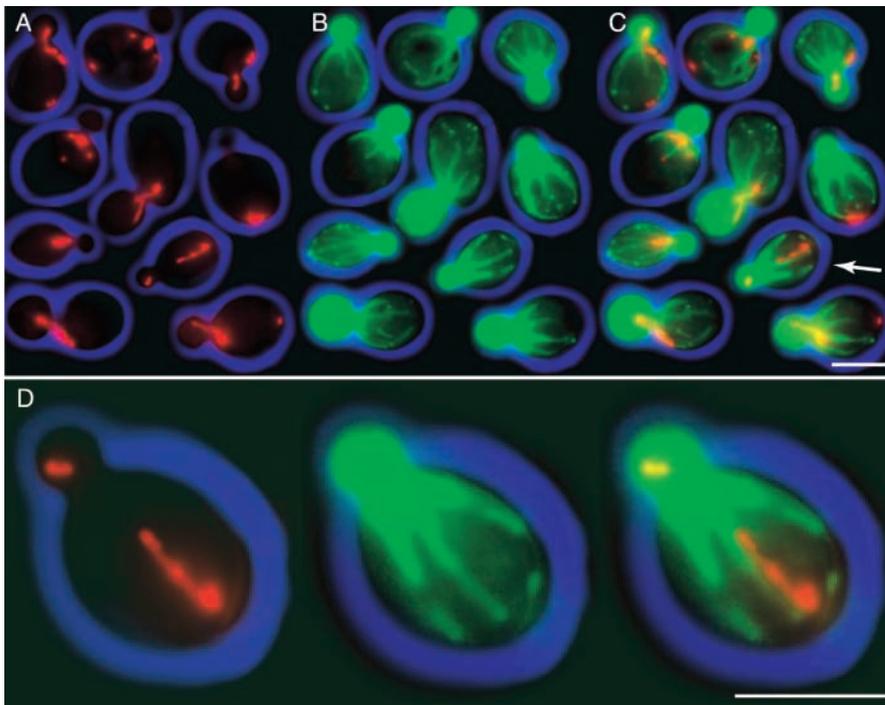
Figure 7. **Colocalization study of peroxisomes and actin cables in *vps1Δ* cells.** GFP-PTS1–labeled (A) log phase cells were fixed and the actin cytoskeleton stained with phalloidin-rhodamine (B) and the two channels were overlaid to check for colocalization (C). Peroxisomes are almost exclusively localized on actin cables. The long peroxisomal tubules typical for *vps1Δ* cells orient along actin cables. This is especially apparent in the cell indicated with an arrow and represented in larger magnification in D. Bars, 5 μm.

most likely candidates for involvement in peroxisome segregation. They consist of an NH₂-terminal motor domain, a neck domain, a coiled-coiled domain involved in dimerization, and a COOH-terminal cargo binding domain (Cheney et al., 1993; for reviews see Hildebrandt and Hoyt, 2000; Reck-Peterson et al., 2000). The two class V myosins in *S. cerevisiae* are named Myo2 and Myo4p. Myo2 is an essential protein. Analyses of temperature-sensitive *MYO2* alleles have shown that Myo2 is directly involved in vesicular transport, vacuolar inheritance, and nuclear spindle orientation (Johnston et al., 1991; Govindan et al., 1995; Hill et al., 1996; Santos and Snyder, 1997; Catlett and Weisman, 1998; Schott et al., 1999; Beach et al., 2000; Yin et al., 2000). Myo4 is required for transport of specific mRNAs
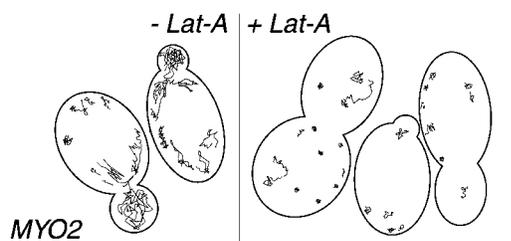
from the mother cell to the daughter cell (Bobola et al., 1996; Long et al., 1997; Takizawa et al., 1997). We expressed GFP-PTS1 in wild-type *MYO2*, *myo2–12*, *myo2–16*, *myo2–20*, *myo2–66*, and *myo4Δ* mutants (Johnston et al., 1991; Schott et al., 1999).

myo2–66 cells already at the permissive temperature were shown to be defective in vacuolar dynamics (Catlett and Weisman, 1998). When analyzing the localization of peroxisomes in the *myo2–66* cells we observed a striking delay in insertion of peroxisomes into the bud (Fig. 9). 87% of all small-budded *myo2–66* cells lacked peroxisomes in the bud, whereas this was the case in only 12% of wild-type cells (*n* = 250). Analysis of the other *myo2-ts* and the *myo4Δ* cells did not show significant alterations in tip localization of peroxisomes.

In addition, we tracked peroxisomal dynamics over a time interval of 15 min in the *myo2-ts* mutants at 24°C and after 10 min of incubation at 37°C. Typical examples of peroxisomal tracks are depicted in Fig. 10. Wild-type cells showed indistinguishable dynamics at both temperatures similar to those described above. This was completely different when analyzing the dynamics of the *myo2-ts* cells. At 24°C peroxisomal distribution appeared indistinguishable from wild-type and fast movements occurred frequently in the buds, but at 37°C only minor oscillations of peroxisomes were detectable. This effect is reversible as cells shifted back to 24°C for 30 min resulted again in normal peroxisome movement. In contrast to the *myo2-ts* mutants, the *myo4Δ* mutant did not display any observable alterations in peroxisomal dynamics. We conclude that peroxisomes migrate along actin cables using the class V myosin, Myo2.

Discussion

During the cell cycle, organelles must be accurately multiplied and partitioned to daughter cells (Nunnari and Walter,

Figure 8. **Analysis of Lat-A on peroxisomal dynamics by tracking of peroxisomal movements for 15 min in wild-type cells.** In cells not treated with Lat-A, highly dynamic peroxisomal movements can be observed that are described in more detail in Fig. 1 C. After Lat-A incubation, peroxisomal translocations are abolished and only oscillations persist. A few peroxisomes show nondirected translocations, probably due to detachment from the cell cortex and passive cytoplasmic movement. Tracking of peroxisomes was based on a 15 min time-lapse sequence with acquisition intervals of 15 s as shown for Video 9, available at http://www.jcb.org/cgi/content/full/jcb.200107028/DC1. In total, 10 Lat-A and 10 control cells have been analyzed with similar results.

Figure 9. **Peroxisome distribution in small budded cells at 24°C as seen in GFP-PTS–labeled wild-type and *myo2–66* cells.** (A) Peroxisome insertion into the nascent bud at very early stages is typical for wild-type cells. (B) In the *myo2–66* mutant most cells do not localize peroxisomes into the bud at early cell cycle stages. In addition, the cells accumulate fluorescent vacuoles not observed in the wild-type cells. Bar, 5 μm.
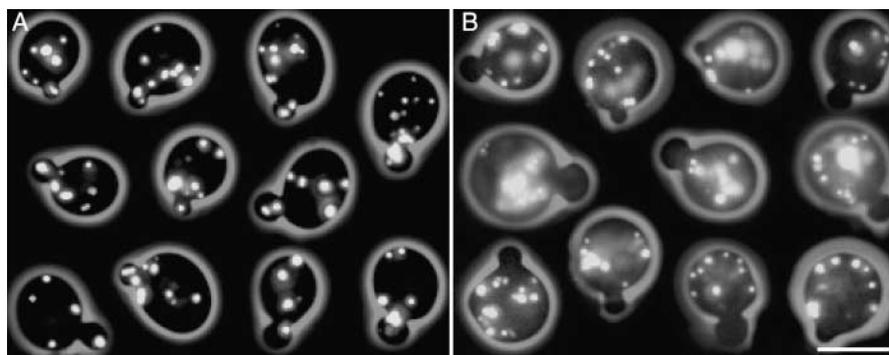
1996; Warren and Wickner, 1996; Yaffe, 1999). This is particularly so for the autonomously replicating organelles comprising nucleus/ER, mitochondria, and chloroplasts. Although other organelles comprising Golgi complex, endosomes, lysosomes/vacuole, and secretory vesicles are derived from the ER it becomes increasingly clear that special care is taken to ensure their efficient segregation too. Here we have shown that peroxisomes follow the same rule. Peroxisomes were visualized by transforming yeast cells with a gene coding for GFP with the PTS1 appended to its COOH terminus, which is efficiently imported into the organelles. This allowed us to follow their partitioning between mother and daughter cells for several generations by time-lapse microscopy. Under the conditions of growth cells maintained on average a number of nine peroxisomes. This apparently involves an active fission process that results in the formation of additional peroxisomes. We infer this from our observation that most cells with a deleted *VPS1* gene maintain only a single enlarged peroxisome. Vps1p is a member of the dynamin protein family whose members are known to function in vesicle trafficking events involving the ability to constrict and sever membrane tubules into discrete vesicles (van der Bliek, 1999; McNiven et al., 2000). In yeast, Dnm1p

and Mgm1p participate in fission of mitochondria (Otsuga et al., 1998; Sesaki and Jensen, 1999; Shepard and Yaffe, 1999; Mozdy et al., 2000; Tieu and Nunnari, 2000; Wong et al., 2000), whereas Vps1p is required for sorting of proteins to the vacuole (Rothman et al., 1990; Wilsbach and Payne, 1993). It is interesting that mitochondria, with their endosymbiont history, have their own dedicated dynamins, whereas peroxisomes share a dynamin-like function with the vacuolar compartment. It adds additional thought to recent ideas that peroxisomes are semiautonomous organelles which are at least in part dependent on contributions from the ER (Titorenko and Rachubinski, 1998). This contribution may be particularly important in terms of donating the phospholipid membranes to the peroxisomal compartment.

The constant number of peroxisomes per cell, the correct segregation of peroxisomes to the buds, and the rather precise control over the number of peroxisomes retained by the mother and delivered to the bud suggest the existence of various components taking part in peroxisome partitioning. In this respect, peroxisomes resemble mitochondria. Here a "retention zone" in the mother cell distal from the bud was defined in which a subset of mitochondria was retained by interaction with the actin cytoskeleton (Yang et al., 1999). Precise partitioning is even more obvious in the *vps1Δ* mutant. In all cases we observed that the single remaining peroxisome was partitioned equally well between mother and daughter. Whether this is achieved by a remaining fission capacity of another protein than Vps1p or is in part an indirect, physical effect of pulling forces acting from opposite sites remains to be studied.

Moreover, during our time-lapse analysis it became apparent that in a few *vps1Δ* mutant cells early insertion of the peroxisomal compartment failed. These cells showed a striking delay in cytokinesis compared with the other cells in the time-lapse sequence. This observation is similar to those made in some *mdm* and *vac* mutants (Weisman et al., 1990; McConnell and Yaffe, 1993; Xu and Wickner, 1996). This suggests the existence of a surveillance mechanism preventing the onset of cytokinesis until all organelles are properly partitioned. The conditional dependency of *S. cerevisiae* cells on peroxisomes and the reduced number of peroxisomes in the *vps1Δ* mutant could provide a valuable basis for genetic screens to identify putative components of such an organelle checkpoint mechanism.

We have studied the interaction of Vps1p with peroxisomes using a Vps1-YFP fusion protein and CFP-marked peroxisomes. Microscopic analysis of the double-labeled cells showed moderate cytoplasmic localization of the Vps1-YFP
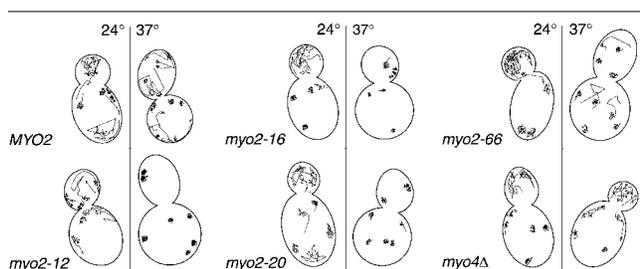

Figure 10. **Analysis of peroxisomal dynamics in GFP-PTS1–labeled *MYO2*, *myo2-ts*, and *myo4Δ* cells at 24°C and 37°C by tracking of peroxisomal movements for 15 min.** In all strains at 24°C, highly dynamic peroxisomal movements can be observed that are described in more detail in Fig. 1 C. At 37°C, *MYO2* wild-type and *myo4Δ* deletion mutants exhibit peroxisomal movements similar to those observed at 24°C. The other mutants show significantly reduced peroxisomal translocations at 37°C and only minor oscillations are observable. A few peroxisomes in the *myo2–66* mutants show nondirected translocations, probably due to detachment from the cell cortex and passive cytoplasmic random movement. Tracking of peroxisomes was based on 15 min time-lapse sequence with acquisition intervals of 15 s. 10 individual cells of each mutant at both temperatures have been analyzed and representative examples are shown in this figure.

protein with additional spotted accumulations, most likely in the Golgi and post-Golgi compartments as suggested in the literature (Rothman et al., 1990). Due to the disperse localization of Vps1p, minor fractions always seemed to colocalize with peroxisomes. Coordinated movement of Vps1p with individual peroxisomes occurred and persisted for several minutes. We surmise that Vps1p only transiently interacts with peroxisomes and that fission events of peroxisomes can occur without accumulation of high concentrations of the Vps1 protein at the peroxisome membrane.

The orderly, track-like movements of peroxisomes in dividing wild-type cells suggested the involvement of cytoskeletal components. All our evidence indicates that peroxisomes are bound in the mother cell by the cortical actin skeleton and that they actively slide along actin filaments to the site of bud appearance and subsequently into the bud itself. Our time lapse analyses of Cap2-YFP, CFP-PTS1–labeled cells revealed directed peroxisomal movement relative to the Cap2-labeled actin patches along the cell cortex strictly following the polarity of the actin cytoskeleton. In fixed cells stained for actin, all the GFP-PTS1 fluorescently labeled peroxisomes colocalize with actin polymers. The dynamic movements of peroxisomes in life cells were lost upon treatment of the cells with Lat-A, a poison that breaks down actin filaments. Finally, the protein responsible for tracking of peroxisomes through the cell is Myo2, a typical actin-based motor protein. This was inferred from the behavior of several thermosensitive alleles of Myo2. In all cases dynamic movements of peroxisomes stopped after bringing the cells to the nonpermissive temperature. In contrast, the movements were unaffected when wild-type or a Myo4p deletion mutant were inspected under the same conditions. Moreover, no colocalization of peroxisomes with the microtubule cytoskeleton was observed nor was any effect noted in a mutant (*spc72Δ*) unable to form astral microtubules, which obviates the need for other motor proteins than Myo2p. Together, these results indicate that partitioning of peroxisomes between mother and bud is dependent on the actin cytoskeleton and an actin-specific motor protein. In analogy to mitochondria retention of a subset of peroxisomes in the mother cell may also require actin, suggesting a dual role for the actin cytoskeleton.

Myo2p has also been implicated in vectorial transport of secretory vesicles, late Golgi compartment, and the vacuole to the emerging bud (Johnston et al., 1991; Govindan et al., 1995; Hill et al., 1996; Catlett and Weisman, 1998; Schott et al., 1999; Karpova et al., 2000; Rossanese et al., 2001). Selectivity in recognizing the vacuolar cargo was ascribed to the myosin tail (Catlett and Weisman, 1998, 2000). For instance, a number of mutations defined a short region that was required for specific binding to the vacuole. It will be interesting to explore whether a similar tail region can be defined for binding to peroxisomes and to find out which peroxisomal membrane protein is the target for Myo2p interaction. This is also of clinical interest. There is a great latitude in loss of peroxisome function before organismal life is compromised. As a result, a number of diseases are known that are caused by diminished or even complete absence of peroxisome function. Considering the above mentioned specificity in Myo2p tail function and the predicted existence of a peroxisome-specific interaction partner, it is reasonable to expect that deficiencies of the corresponding homologs in humans can be the cause of disease. This prediction is supported by the occurrence of Griscelli disease (Pastural et al., 1997; Menasche et al., 2000; Wilson et al., 2000). Some forms of this syndrome are due to mutations in the human Myosin-Va protein, a homologue of yeast Myo2p. A mutation resulting in truncation of the protein after the motor domain and an amino acid substitution in front of the globular tail domain were reported. It will be interesting to study the behavior of peroxisomes in Griscelli patient cells and to test if similar diseases related to (partial) loss of peroxisome function exist. Further research in yeast can help to reveal the severity of the phenotypes resulting from mutations in proteins of the peroxisome segregation machinery and may help to predict how such diseases might present themselves in patients.

Materials and methods

Strains, media, and yeast transformation

Yeast strains used in this study are listed in Table I. Yeast media were prepared as described by Guthrie and Fink (1991). The yeast transformation procedure was based on the protocol by Schiestl and Gietz (1989). After the heat shock step, cells were pelleted and resuspended in 5 ml of YPD and incubated for 2 h at 30°C. Cells were again pelleted, resuspended in 1 ml H$_2$O and plated on selective YPD-G418 medium (200 mg/l geneticin). Lat-A (Molecular Probes) was added from a 200 mM stock in DMSO to exponentially growing YPD cultures (final concentration 200 μM). Further incubation for 15 min at 30°C was performed on a roller drum and the cells then analyzed by microscopy. *E. coli* XL1-blue (Bullock et al., 1987) was used to propagate plasmids.

DNA manipulations, cloning procedures, and strain constructions

DNA manipulations were performed as described by Sambrook et al. (1989). We applied a PCR-based method to construct gene deletion cassettes for transformations (Wach et al., 1994). DNA of *E. coli* plasmids pFA6-KanMX4 (Wach et al., 1994) and pFA6a-YFP-His3MX6 (Yeast Resource Center) served as template for preparative PCR reactions. Genomic integration of the corresponding construct was verified by analytical PCR (Huxley et al., 1990; Wach et al., 1994). Yeast strains were grown on YPD-G418 (200 mg/l geneticin) to select for transformants that had integrated kanMX4, or GFP-kanMX6 cassettes. Growth on SD plates lacking histidine, leucine, or tryptophane selected for YFP-HIS3MX6 or YIplac derived construct (see below) integration.

Plasmids pEW161, pEW171, and pEW213 were constructed as follows. pEW161: PCR amplification of the *HIS3* promoter with 5′-GGGAATTC-TATTACTCTTGGCCTCCTC-3′ introducing an EcoR1 site at the 5′ end and a SacI site at the 3′ end with primer 5′-GCAAGATAAACGAAGGCAAAG-3′. The fragment was subsequently introduced into YIplac204 (Gretz and Sugino) (pEW156) and YIplac211 (pEW157). GFP-PTS1 (from pEW88; Hettema et al., 1998) was cloned into pEW156 and pEW157 cut with BamHI and HindIII resulting in pEW160 and pEW161, respectively. pEW171: the NcoI-BstBI fragment GFP-PTS1 derived from pEW160 was swapped with that of CFP or YFP. pEW213: genomic Vps1 was PCRed with primer 5′-GGATAGTATGATAGCTTCAGAG-3′ and primer 5′-GGGCTGCAGAACAGAGGAGACGATTTGATAG-3′ amplifying its promoter, the *VPS1* gene without the stop codon and introducing a PstI site. This fragment has been ligated in frame with YFP in YIplac211 using EcoR1 and PstI.

For gene deletions we followed the EUROFAN guidelines (guidelines for EUROFAN B0 program ORF deletants, plasmid tools, and basic functional analyses are available at www.mips.biochem.mpg.de/proj/eurofan/index.html) for gene replacement in *S. cerevisiae*. We used the oligonucleotide pairs depicted in Table II for generation of the KanMX4, deletion cassettes, or YFP fusion constructs. To label microtubules we integrated plasmid pAFS125 into the *ura3Δ1* locus (Straight et al., 1997). To label peroxisomes we integrated pEW161 or pEW177 into the *ura3* or pEW171 into the *trp1* locus. Microtubules or peroxisomes were clearly observable under the fluorescence microscope upon successful transformation. Label-

Table I. **Yeast strains used in this study**

Strain	Genotype	Source
BJ1991	*MAT_ ura3-251 leu2 trp1 prb1-1122 pep4-3 gal2*	Jones, 1977
BSL1-2c	*MATa ura3_ His4-519 leu2-3 leu2-112*	B. Lemire
FY 1679	*MATα/a ura3-52Δ1/ura3-52Δ1 trp1Δ63/TRP1 leu2Δ1/LEU2 his3Δ200/HIS3*	B. Dujon
DHY 339	*MAT_ ura3-251::GFP-PTS1-URA3(pEW161) trp1 leu2 prb1-1122 pep4-3 gal2*	This study
DHY 340	*MAT_ vps1_::kanMX4 ura3-251::GFP-PTS1-URA3(pEW161) trp1 leu2 prb1-1122 pep4-3 gal2*	This study
DHY 341	*MAT_ ura3-251::VPS1-YFP1-URA3(pEW 213) trp1 leu2 prb1-1122 pep4-3 gal2*	This study
DHY 342	*MAT_ vps1_::kanMX4 ura3-251::VPS1-YFP1-URA3(pEW231) trp1 leu2 prb1-1122 pep4-3 gal2*	This study
DHY 343	*MAT_ ura3-251::VPS1-YFP-URA3(pEW213) trp::CFP-PTS1-TRP1(pEW171) leu2 prb1-1122 pep4-3 gal2*	This study
DHY 344	*MAT_ vps1_::kanMX4 ura3-251::VPS1-YFP-URA3(pEW213) trp::CFP-PTS1-TRP1(pEW171) leu2 prb1-1122 pep4-3 gal2*	This study
DHY 345	*MATα CAP2::YFP-HIS3MX4 ura3-52Δ1::CFP-PTS1-URA3(pEW177) trp1Δ63 leu2Δ1 his3Δ200*	This study
DHY 346	*MATα CAP2::YFP-HIS3MX4 ura3-52Δ1::CFP-PTS1-URA3(pEW177) trp1Δ63 leu2Δ1 his3Δ200*	This study
DHY 347	*MATα ura3-52Δ1::GFP-Tub1-URA3(pAFS125) leu2Δ1::YFP-PTS1-LEU2 trp1Δ63 his3Δ200*	This study
DHY 348	*MATα/a ura3-52Δ1::CFP-PTS1-URA3(pEW177)/ura3-52Δ1::CFP-PTS1-URA3(pEW177) CAP2::YFP-HIS3MX4/CAP2::YFP-HIS3MX4 trp1Δ63/ trp1Δ63 leu2Δ1/leu2Δ1 his3Δ200/his3Δ200*	This study
DHY 349	*MATα/a vps1_::kanMX4/vps1_::kanMX4 ura3-251::GFP-PTS1-URA3(pEW161)/ ura3_ TRP1/trp1 leu2/ leu2-112 PRB1/prb1-1122 PEP4/pep4-3 GAL2/gal2*	This study
DHY350	*MAT_ ura3-2512::GFP-PTS1-URA3(pEW161) leu2 trp1 prb1-1122 pep4-3 gal2*	This study
DHY 351	*MATα ura3_2::GFP-PTS1-URA3(pEW161) His4-519 leu2-3 leu2-112*	This study
ABY 530	*MAT_ his3_200::myo2-20-HIS3 ura3-52 leu2-3,112 lys2-801 ade2-101 Gal1*	Schott et al., 1999
ABY 531	*MAT_ his3_200::MYO2-HIS3 ura3-52 leu2-3,112 lys2-801 ade2-101 Gal1*	Schott et al., 1999
ABY 532	*MAT_ his3_200::myo2-12-HIS3 ura3-52 leu2-3,112 lys2-801 ade2-101 Gal1*	Schott et al., 1999
ABY 535	*MAT_ his3_200::myo2-66-HIS3 ura3-52 leu2-3,112 lys2-801 ade2-101 Gal1*	Schott et al., 1999
ABY 536	*MAT_ his3_200::myo2-16-HIS3 ura3-52 leu2-3,112 lys2-801 ade2-101 Gal1*	Schott et al., 1999
ABY 538	*MAT_ his3_200::myo2-18-HIS3 ura3-52 leu2-3,112 lys2-801 ade2-101 Gal1*	Schott et al., 1999
DHY 353	*MAT_ his3_200::myo2-20-HIS3 ura3-52::GFP-PTS1-URA3(pEW161) leu2-3,112 lys2-801 ade2-101 Gal1*	This study
DHY 354	*MAT_ his3_200::MYO2-HIS3 ura3-52::GFP-PTS1-URA3(pEW161) leu2-3,112 lys2-801 ade2-101 Gal1*	This study
DHY 355	*MAT_ his3_200::myo2-12-HIS3 ura3-52::GFP-PTS1-URA3(pEW161) leu2-3,112 lys2-801 ade2-101 Gal1*	This study
DHY 356	*MAT_ his3_200::myo2-66-HIS3 ura3-52::GFP-PTS1-URA3(pEW161) leu2-3,112 lys2-801 ade2-101 Gal1*	This study
DHY 357	*MAT_ his3_200::myo2-16-HIS3 ura3-52::GFP-PTS1-URA3(pEW161) leu2-3,112 lys2-801 ade2-101 Gal1*	This study
DHY 358	*MAT_ his3_200::myo2-18-HIS3 ura3-52::GFP-PTS1-URA3(pEW161) leu2-3,112 lys2-801 ade2-101 Gal1*	This study
DHY 370	*MATα spc72_::KanMX4 ura3-52::GFP-PTS1-URA3(pEW161) trp1Δ63 leu2Δ1 his3Δ200*	This study

ing of Vps1 was performed by integrating pEW213 into the *ura3* locus. Correct integration rescued the peroxisomal morphology defect and the temperature sensitivity of *vps1Δ* strains.

Microtubule depolymerization
Microtubules were depolymerized by adding 2.5 μl/ml culture of a 5 mg/ml stock solution of either nocodazole or benomyl (both Sigma-Aldrich) solved in DMSO. After 90 min incubation at 30°C, most cells arrested with a single large bud. In drug-treated cells with GFP-labeled microtubules, no microtubules could be identified, whereas a normal array of microtubules was present in DMSO-treated control cells.

Acquisition of still images
YFP-PTS1, CFP-PTS1, Cap2-YFP, and GFP-Tub1–labeled wild-type and *spc72Δ* strains were grown in YPD medium to early log phase at 30°C, 3 μl of the culture were spread on a poly-L-lysine–treated slide overlaid with a coverslip and immediately used for microscopy. To simultaneously visualize peroxisomes and the actin cytoskeleton, GFP-PTS1 cells were grown in 25 ml of YPD at 30°C to early log phase and then fixed and stained (Amberg, 1998) using modifications to preserve GFP fluorescence: the first formaldehyde fixation was reduced to 5 min, the second to 30 min, and the rhodamine-phalloidin staining time to 30 min. It was essential to keep the pH above 8.0. Subsequently, the cells were immediately used for analysis. We acquired five z-axis planes spaced by 0.8 μm. In each z-axis plane we acquired one GFP and one rhodamine image using a Plan-Neofluar 100×, 1.3 oil, PH3 objective and a 2× Optovar (ZEISS) with 5 s exposure times, 100% fluorescence transmission. Each individual plane was then processed using the two-dimensional deconvolution algorithm of the AutoDeblur software (AutoQuant Imaging). Separately, the GFP and rhodamine images where then averaged into one plane, scaled, and converted to 8-bit images. We used different scaling parameters for the mother cell bodies and buds of rhodamine channel–acquired images due to the much weaker signal of the actin cables in the mother cell compared with the patches in the bud. Finally, the phase-contrast, GFP, and rhodamine images were overlaid using Metamorphs "Overlay" function with default color balance settings using false color settings as depicted in the figure legend.

In vivo microscopy procedures and techniques
The video microscopy setup and in vivo time lapse procedures using GFP-PTS1, CFP-PTS1, Cap2-YFP, and GFP-Tub1–labeled strains were described by Hoepfner et al. (2000). Imaging of the YFP/CFP variant of GFP was performed using filter sets 41028 and 31044v2 (Chroma Technology Corp.). For long term in vivo time-lapses we used diploid cells because spreading of the cells was better due to bipolar budding. Acquisition settings like interval time, exposure time, excitation light transmission, the number, and spacing of the z-axis planes are indicated in the video legends. To analyze the temperature-sensitive mutants at the nonpermissive temperature we used a temperature-adjustable stage (Biowerk). Acquisition and processing

Table II. **Oligonucleotides used in this work**

vps1Δ1	5′-ACCAAAATAAGGACCGTACGAAAACTGCACATTTTATATTATCAGATATCGCTTCGTACGCTGCAGGTCGAC-3′
	5′-AACAGAGGAGACGATTTGACTAGCGTTTCTCAATATCTCGACCATCTCATCGATGAATTCGAGCTCG-3′
spc72Δ1	5′-AACACTAATATCAAAAAACTAAGCAAACAACATAAGGAAAGTTATAGCCGCTTCGTACGCTGCAGGTCG-3′
	5′-AGAGTGACTGAGTGTTACATTAAATATATTTATATATAAACGTATGATATATCATCGATGAATTCGAGCTCGTT-3′
Cap2Fus	5′-GAAGCGAATAAAGACGCACAGGCAGAGGTAATCAGAGGTTTACAGTCTTTAGGTCGACGGATCCCCGGGTT-3′
	5′-CACTTAGTGCTGCTCTATGTATTTATATGATATACCAGCGATACATGTAACATCGATGAATTCGAGCTCG-3′

of images was performed using the Metamorph 4.1 program (Universal Imaging Corp.). Acquired z-axis stacks were merged into one plane using the "stack arithmetic: maximum" command of Metamorph. Stored images were then scaled and converted to 8-bit files. False color look-up tables were assigned to the individual channels as indicated in the figure legends. The phase-contrast and fluorescence 8-bit planes were then overlaid using the built-in "Overlay" command with default color balance.

Online supplemental material

For time-lapse analysis we assembled the picture files to videos in QuickTime format (Apple Computer) with a frame rate of 10 frames per second using the Premiere 4.2 program (Adobe Systems Europe). The videos are platform-independent and can be viewed using QuickTime movie player that can be downloaded at www.apple.com. Explanatory remarks and detailed information about acquisition settings are shown in the individual video legends associated with the figures showing representative still images of the time-lapse sequences. Videos are available at http://www.jcb.org/cgi/content/full/jcb.200107028/DC1.

References

Adams, A.M., and J.R. Pringle. 1984. Relationship of actin and tubulin distribution to bud growth in wild-type and morphogenetic mutant *Saccharomyces cerevisiae*. *J. Cell Biol.* 98:934–945.

Amberg, D.C. 1998. Three-dimensional imaging of the yeast actin cytoskeleton through the budding cell cycle. *Mol. Biol. Cell.* 9:3259–3262.

Beach, D.L., J. Thibodeaux, P. Maddox, E. Yeh, and K. Bloom. 2000. The role of the proteins Kar9 and Myo2 in orienting the mitotic spindle of budding yeast. *Curr. Biol.* 10:1497–1506.

Bobola, N., R.P. Jansen, T.H. Shin, and K. Nasmith. 1996. Asymmetric accumulation of Ash1p in postanaphase nuclei depends on a myosin and restricts yeast mating-type switching to mother cells. *Cell.* 84:699–709.

Bretscher, A., B. Drees, E. Harsay, D. Schott, and T. Wang. 1994. What are the basic functions of microfilaments? Insights from studies in budding yeast. *J. Cell Biol.* 126:824–825.

Brocard, L., G. Lametschandter, R. Koudelka, and A. Hartig. 1997. Pex14p is a member of the protein linkage map of Pex5p. *EMBO J.* 16:5497–5500.

Brown, S.S. 1997. Myosins in yeast. *Curr. Opin. Cell Biol.* 9:44–48.

Bullock, W.O., J.M. Fernandez, and J.M. Short. 1987. XLI-Blue: A high efficiency plasmid transforming recA *Escherichia coli* strain with β-galactosidase selection. *Biotechniques.* 5:376–378.

Byers, B. 1981. Cytology of the yeast life cycle. The molecular biology of the yeast *Saccharomyces*. Life cycle and inheritance. Cold Spring Harbor Laboratory Press, Cold Spring Harbor, NY. 59–96.

Byers, B., and L. Goetsch. 1975. Behaviour of spindle and spindle plaques in the cell cycle and conjugation of *Saccharomyces cerevisiae*. *J. Bacteriol.* 124:511–523.

Carminati, J.L., and T. Stearns. 1997. Microtubules orient the mitotic spindle through dynein-dependent interactions with the cell cortex. *J. Cell Biol.* 138:629–641.

Catlett, N.L., and L.S. Weisman. 1998. The terminal tail region of a yeast myosin-V mediates its attachment to vacuole membranes and sites of polarized growth. *Proc. Natl. Acad. Sci. USA.* 95:14799–14804.

Catlett, N.L., and L.S. Weisman. 2000. Divide and multiply: organelle partitioning in yeast. *Curr. Opin. Cell Biol.* 12:509–516.

Chen, X.P., H. Yin, and T.C. Huffaker. 1998. The yeast spindle pole body component Spc72p interacts with Stu2p and is required for proper microtubuli assembly. *J. Cell Biol.* 141:1169–1179.

Cheney, R.E., M.K. O'Shea, J.E. Heuser, M.V. Coelho, J.S. Wolenski, E.M. Espreafico, P. Forscher, P.E. Larson, and M.S. Mooseker. 1993. Brain myosin-V is a two-headed unconventional myosin with motor activity. *Cell.* 75:13–23.

Coue, M., S.L. Brenner, I. Spector, and E.D. Korn. 1987. Inhibition of actin polymerization by latrunculin A. *FEBS Lett.* 213:316–318.

Doyle, T., and D. Botstein. 1996. Movement of yeast cortical actin cytoskeleton visualized in vivo. *Proc. Natl. Acad. Sci. USA.* 93:3886–3891.

Erdmann, R., M. Veenhuis, and W.H. Kunau. 1997. Peroxisomes: organelles at the crossroads. *Trends Cell Biol.* 7:400–407.

Ford, S.K., and J.R. Pringle. 1991. Cellular morphogenesis in the *Saccharomyces cerevisiae* cell cycle: localization of the CDC11 gene product and the timing of the events at the budding site. *Dev. Genet.* 12:281–292.

Govindan, B., R. Bowser, and P. Novick. 1995. The role of Myo2, a yeast class V myosin, in vesicular transport. *J. Cell Biol.* 128:1055–1068.

Guthrie, C., and G.R. Fink. 1991. Guide to yeast genetics and molecular biology. *Methods Enzymol.* 194:14–15.

Hettema, E.H., C.C. Ruigrok, M.G. Koerkamp, M. van den Berg, H.F. Tabak, B. Distel, and I. Braakman. 1998. The cytosolic DnaJ-like protein Djp1p is involved specifically in peroxisomal protein import. *J. Cell Biol.* 142:421–434.

Hettema, E.H., B. Distel, and H.F. Tabak. 1999. Import of proteins into peroxisomes. *Biochim. Biophys. Acta.* 1451:17–34.

Hettema, E.H., W. Girzalsky, M. van den Berg, R. Erdmann, and B. Distel. 2000. *Saccharomyces cerevisiae* Pex3p and Pex19p are required for proper localization and stability of peroxisomal membrane proteins. *EMBO J.* 19:223–233.

Hildebrandt, E.R., and A.M. Hoyt. 2000. Mitotic motors in *Saccharomyces cerevisiae*. *Biochim. Biophys. Acta.* 1496:99–116.

Hill, K.L., N.L. Catlett, and L.S. Weisman. 1996. Actin and myosin function in directed vacuole movement during cell division in *Saccharomyces cerevisiae*. *J. Cell Biol.* 135:1535–1549.

Hoepfner, D., A. Brachat, and P. Philippsen. 2000. Time-lapse video microscopy reveals astral microtubule detachment in the yeast spindle pole mutant *cnm67*. *Mol. Biol. Cell.* 11:1197–1211.

Howard, R.J. 1981. Ultrastructural analysis of hyphal tip cell growth in the spitzenkorper, cytoskeleton and endomembranes after freeze-substitution. *J. Cell Sci.* 48:89–103.

Howard, R.J., and J.R. Aist. 1980. Cytoplasmic microtubules and fungal morphogenesis: ultrastructural effects of methyl benzimidazole-2-yl carbamate determined by freeze–substitution of hyphal tip cells. *J. Cell Biol.* 107:1997–2010.

Huxley, C., E.D. Green, and I. Dunham. 1990. Rapid assessment of *S. cerevisiae* mating type by PCR. *Trends Genet.* 6:236.

Jacobs, C.W., E.M.A. Alison, P.J. Szaniszlo, and J.R. Pringle. 1988. Functions of microtubules in the *Saccharomyces cerevisiae* cell cycle. *J. Cell Biol.* 107:1409–1426.

Johnston, G., J. Pendergast, and R. Singer. 1991. The *Saccharomyces cerevisiae* MYO2 gene encodes an essential myosin for vectorial transport of vesicles. *J. Cell Biol.* 113:539–551.

Jones, E.W. 1977. Proteinase mutants of *Saccharomyces cerevisiae*. *Genetics.* 85:23–33.

Karpova, T.S., S.L. Reck-Peterson, N.B. Elkind, M.S. Mooseker, P.J. Novick, and J.A. Cooper. 2000. Role of actin and Myo2p in polarized secretion and growth of *Saccharomyces cerevisiae*. *Mol. Biol. Cell.* 11:1727–1737.

Kilmartin, J.V., and A.E.M. Adams. 1984. Structural rearrangements of tubulin and actin during the life cycle of the yeast *Saccharomyces cerevisiae*. *J. Cell Biol.* 98:922–933.

Knop, M., and E. Schiebel. 1998. Receptors determine the cellular localization of a gamma-tubulin complex and thereby the site of microtubule formation. *EMBO J.* 17:3952–3967.

Lazarow, P.B., and Y. Fujiki. 1985. Biogenesis of peroxisomes. *Annu. Rev. Cell. Biol.* 1:489–530.

Long, R.M., R.H. Singer, X. Meng, K. Gonzalez, K. Nasmith, and R.P. Jansen. 1997. Mating type switching in yeast controlled by asymmetric localization of *ASH1* mRNA. *Science.* 277:383–387.

Madden, K., and M. Snyder. 1998. Cell polarity and morphogenesis in yeast. *Annu. Rev. Microbial.* 52:687–744.

McConnell, S.J., and M.P. Yaffe. 1993. Intermediate filament formation by a yeast protein essential for organelle inheritance. *Science.* 260:687–689.

McNiven, M.A., and K.R. Porter. 1986. Microtubule polarity confers directions to pigment transport in chromatophores. *J. Cell Biol.* 103:1547–1555.

McNiven, M.A., H. Cao, K.R. Pitts, and Y. Yoon. 2000. The dynamin family of mechanoenzymes: pinching in new places. *Trends Biochem. Sci.* 25:115–120.

Menasche, G., E. Pastural, J. Feldmann, S. Certain, F. Ersoy, S. Dupuis, N. Wulffraat, D. Bianchi, A. Fischer, F. Le Deist, and G. de Saint Basile. 2000. Mutations in RAB27A cause Griscelli syndrome associated with haemophagocytic syndrome. *Nat. Genet.* 25:173–176.

Monosov, E.Z., T.J. Wenzel, H.G. Lüers, J.A. Heyman, and S. Subramani. 1996.

Labeling of peroxisomes with green fluorescent protein in living *P. pastoris* cells. *J. Histochem. Cytochem.* 44:581–589.

Mozdy, A.D., J.M. McCaffery, and J.M. Shaw. 2000. Dnm1p GTPase-mediated mitochondrial fission is a multi-step process requiring the novel integral membrane component Fis1p. *J. Cell Biol.* 151:367–380.

Nunnari, J., and P. Walter. 1996. Regulation of organelle biogenesis. *Cell.* 84:389–394.

Otsuga, D., B.R. Keegan, E. Brisch, J.W. Thatcher, G.J. Hermann, W. Bleazard, and J.M. Shaw. 1998. The dynamin-related GTPase, Dnm1p, controls mitochondrial morphology in yeast. *J. Cell Biol.* 143:333–349.

Palmer, R.E., D.S. Sullivan, T. Huffaker, and D. Koshland. 1992. Role of astral microtubules and actin in spindle orientation and migration in the budding yeast, *Saccharomyces cerevisiae*. *J. Cell Biol.* 119:583–593.

Pastural, E., F.J. Barrat, R. Dufourcq-Lagelouse, S. Certain, O. Sanal, N. Jabado, R. Seger, C. Griscelli, A. Fischer, and G. de Saint Basile. 1997. Griscelli disease maps to chromosome 15q21 and is associated with mutations in the myosin-Va gene. *Nat. Genet.* 16:289–292.

Purdue, P.E., and P.B. Lazarow. 1994. Peroxisomal biogenesis: multiple pathways of protein import. *J. Biol. Chem.* 269:30065–30068.

Rapp, S., R. Saffrich, U. Jakle, W. Ansorge, K. Gorgas, and W.W. Just. 1996. Microtubule-mediated peroxisomal saltations. *Ann. NY Acad. Sci.* 804:666–668.

Reck-Peterson, S.L., D.W. Provance, M.S. Mooseker, and J.A. Mercer. 2000. Class V myosins. *Biochim. Biophys. Acta.* 1496:36–51.

Rindler, M.J., I.E. Ivanov, and D.D. Sabatini. 1987. Microtubule-acting drugs lead to the nonpolarized delivery of the influenza hemagglutinin to the cell surface of polarized Madin-Darby canine kidney cells. *J. Cell Biol.* 104:231–241.

Rogalski, A.A., J.E. Bergamann, and S.J. Singer. 1984. Effect on microtubule assembly status on the intracellular processing and surface expression of an integral protein of the plasma membrane. *J. Cell Biol.* 99:1101–1109.

Rossanese, O.W., C.A. Reinke, B.J. Bevis, A.T. Hammond, I.B. Sears, J. O'Connor, and B.S. Glick. 2001. A role for actin, Cdc1p, and Myo2p in the inheritance of late Golgi elements in *Saccharomyces cerevisiae*. *J. Cell Biol.* 153:47–62.

Rothman, J.H., C.K. Raymond, T. Gilbert, P.J. O'Hara, and T.H. Stevens. 1990. A putative GTP binding protein homologous to interferon-inducible Mx proteins performs an essential function in yeast protein sorting. *Cell.* 61:1063–1074.

Sambrook, J., E.F. Fritsch, and T. Maniatis. 1989. Molecular Cloning: A Laboratory Manual, 2nd Ed. Cold Spring Harbor Laboratory Press, Cold Spring Harbor, NY.

Santos, B., and M. Snyder. 1997. Targeting of chitin synthase 3 to polarized growth sites in yeast requires Chs5p and Myo2p. *J. Cell Biol.* 136:95–110.

Schiestl, R.H., and R.D. Gietz. 1989. High efficiency transformation of intact yeast cells using single stranded nucleic acids as a carrier. *Curr. Genet.* 16:339–346.

Schliwa, M. 1984. Mechanisms of intracellular organelle transport. *In* Cell and Muscle Motility, 5. The Cytoskelton. J.W. Shay, editor. Plenum Press, New York. 1–82.

Schott, D., J. Ho, D. Pruyne, and A. Bretscher. 1999. The COOH-terminal domain of Myo2, a yeast myosin V, has a direct role in secretory vesicle targeting. *J. Cell Biol.* 147:791–807.

Sellers, J.R. 2000. Myosins: a diverse superfamily. *Biochim. Biophys. Acta.* 1496:3–22.

Sesaki, H., and R.E. Jensen. 1999. Division versus fusion: Dnm1p and Fzo1p antagonistically regulate mitochondrial shape. *J. Cell Biol.* 147:699–706.

Shaw, S.L., E. Yeh, P. Maddox, E.D. Salmon, and K. Bloom. 1997. Astral microtubule dynamics in yeast: a microtubule-based searching mechanism for spindle orientation and nuclear migration into the bud. *J. Cell Biol.* 139:985–994.

Shepard, K.A., and M.P. Yaffe. 1999. The yeast dynamin-like protein, Mgm1p, functions on the mitochondrial outer membrane to mediate mitochondrial inheritance. *J. Cell Biol.* 144:711–720.

Soûès, S., and I.R. Adams. 1998. SPC72: a spindle pole component required for spindle orientation in the yeast *Saccharomyces cerevisiae*. *J. Cell Sci.* 111:2809–2818.

Steinberg, G. 1998. Organelle transport and molecular motors in fungi. *Fungal Genet. Biol.* 24:161–177.

Straight, A.F., W.F. Marshall, J.W. Sedat, and A.W. Murray. 1997. Mitosis in living yeast: anaphase A but not metaphase plate. *Science.* 277:574–578.

Subramani, S., A. Koller, and W.B. Snyder. 2000. Import of peroxisomal matrix and membrane proteins. *Annu. Rev. Biochem.* 69:399–418.

Sullivan, D.S., and T.C. Huffaker. 1992. Astral microtubules are not required for anaphase B in *Saccharomyces cerevisiae*. *J. Cell Biol.* 119:379–388.

Tabak, H.F., I. Braakman, and B. Distel. 1999. Peroxisomes: simple in function but complex in maintenance. *Trends Cell Biol.* 9:447–453.

Takizawa, P.A., A. Sil, J.R. Swedlow, I. Herskowitz, and R.D. Vale. 1997. Actin-dependent localization of an RNA encoding a cell-fate determinant in yeast. *Nature.* 389:90–93.

Tieu, Q., and J. Nunnari. 2000. Mdv1p is a WD repeat protein that interacts with the dynamin-related GTPase, Dnm1p, to trigger mitochondrial division. *J. Cell Biol.* 151:353–366.

Tirnauer, J.S., E. O'Toole, L. Berrueta, B.E. Bierer, and D. Pellman. 1999. Yeast Bim1p promotes the G1-spcific dynamics of microtubules. *J. Cell Biol.* 145:993–1007.

Titorenko, V.I., and R.A. Rachubinski. 1998. The endoplasmic reticulum plays an essential role in peroxisome biogenesis. *Trends Biochem. Sci.* 23:231–233.

van der Bliek, A.M. 1999. Functional diversity in the dynamin family. *Trends Cell Biol.* 9:96–102.

van der Bliek, A.M. 2000. A mitochondrial division apparatus takes shape. *J. Cell Biol.* 151:F1–F4.

van den Bosch, H., R.B. Schutgens, R.J. Wanders, and J.M. Tager. 1992. Biochemistry of peroxisomes. *Annu. Rev. Biochem.* 61:157–197.

Vale, R.D., J.M. Scholey, and M.P. Sheetz. 1986. Kinesin: possible biological roles for a new microtubule motor. *Trends Biochem. Sci.* 11:464–468.

Wach, A., A. Brachat, R. Pöhlmann, and P. Philippsen. 1994. New heterologous modules for classical or PCR-based gene disruptions in *Saccharomyces cerevisiae*. *Yeast.* 10:1793–1808.

Waddle, J.A., T.S. Karpova, R.H. Waterston, and J.A. Cooper. 1996. Movement of cortical actin patches in yeast. *J. Cell Biol.* 132:861–870.

Warren, G., and W. Wickner. 1996. Organelle Inheritance. *Cell.* 84:395–400.

Weisman, L.S., S.D. Emr, and W.T. Wickner. 1990. Mutants of *Saccharomyces cerevisiae* that block intervacuole vesicular traffic and vacuole division and segregation. *Proc. Natl. Acad. Sci. USA.* 87:1076–1080.

Wiemer, E.A.C., T. Wenszel, T.J. Deerinck, M.H. Ellisman, and S. Subramani. 1997. Visualization of the paroxysmal compartment in living mammalian cells—dynamic behavior and association with microtubules. *J. Cell Biol.* 136:71–80.

Wilsbach, K., and G.S. Payne. 1993. Vps1p, a member of the dynamin GTPase family, is necessary for Golgi membrane protein retention in *Saccharomyces cerevisiae*. *EMBO J.* 12:3049–3059.

Wilson, S.M., R. Yip, D.A. Swing, T.N. O'Sullivan, Y. Zhang, E.K. Novak, R.T. Swank, L.B. Russell, N.G. Copeland, and N.A. Jenkins. 2000. A mutation in Rab27a causes the vesicle transport defects observed in ashen mice. *Proc. Natl. Acad. Sci. USA.* 97:7933–7938.

Wong, E.D., J.A. Wagner, S.W. Gorsich, J.M. McCaffery, J.M. Shaw, and J. Nunnari. 2000. The dynamin-related GTPase, Mgm1p, is an intermembrane space protein required for maintenance of fusion competent mitochondria. *J. Cell Biol.* 151:341–352.

Xu, Z., and W. Wickner. 1996. Thioredoxin is required for vacuole inheritance in *Saccharomyces cerevisiae*. *J Cell Biol.* 132:787–794.

Yang, H.C., A. Palazzo, T.C. Swayne, and L.A. Pon. 1999. A retention mechanism for distribution of mitochondria during cell division in budding yeast. *Curr. Biol.* 9:1111–1114.

Yaffe, M.P. 1999. Dynamic mitochondria. *Nat. Cell Biol.* 1:E149–E150.

Yin, H., D. Pruyne, T.C. Huffaker, and A. Bretscher. 2000. Myosin V orientates the mitotic spindle in yeast. *Nature.* 406:1013–1015.